

# Two dimensional photonic crystal based 4x2 optical encoder with ultra-compact and high contrast ratio

K. LATHA\*, V. KAVITHA, R. ARUN KUMAR, K. RAMA PRABHA, S. ROBINSON

*Department of Electronic and Communication Engineering, Mount Zion College of Engineering and Technology, Pudukkottai, 622 507, Tamilnadu, India*

Photonic crystal based optical devices is offering high transmission efficiency, more bandwidth and high bit rate for photonic integrated circuits. In this attempt, the proposed two dimensional photonic crystal with triangular lattice based 4x2 encoder is primarily designed using Y Shaped waveguides with line and point defects in order to enhance the functional parameters. By using the Finite Difference Time Domain method (FDTD) and Plane Wave Expansion Method (PWE) method the following parameters such as Normalized Power, Contrast ratio, Response time and Bit rate are estimated. In addition, the impacts of functional parameters while varying the size of the defect rods are explored. The proposed encoder is providing contrast ratio of 13.6 dB, response time of 0.28ps and the bit rate of 3.5Tbps and operated at 1520nm and it can be utilized for high performance optical networks.

(Received March 15, 2021; accepted February 11, 2022)

*Keywords:* Encoder, Photonic band gap, Interference effect, Nonlinear Kerr effect, FDTD, PWE

## 1. Introduction

Optical communication is one of the advanced technologies which create a tremendous impact nowadays. Researcher gives more attention to design optical devices especially in photonic crystals. Photonic Crystal is composed of periodic dielectric or metallo-dielectric nanostructures that have alternate low and high dielectric constant materials. It has three types based on its direction of dielectric constant variation, such as, one, two and three dimensional Photonic Crystal [1]. Among all, 2D Photonic Crystal is most widely used as it supports better confinement of light, easy to control the propagation of light and easy calculation of Band gap and etc. Mainly the optical devices are designed by 2D photonic crystal, such as, Encoders, Decoders [2], Adders [3], Multiplexers and Demultiplexer [4, 5], Isolators [6], Filters [7, 8], Power splitter [9], Directional coupler [10], logic gates [11, 12], Sensors [13] and Switches [14].

The encoder is inevitable device in optical communication which operates based on the logic gate functions. The all optical encoder which mainly designed by using the OR gate function. Fariborz Parandin reported a 2D photonic crystal based 4\*2 encoder [15]. The transmission delay obtained as less than 0.1ps and the contrast ratio as 16.5 dB [16]. Ahmad Mohebzadeh et al. designed a all optical NOT and XOR gate based on interference effect. The contrast ratio and the response time calculated as 19.95 dB and 0.466 ps respectively [17]. Fariborz Parandin reported a simulation of 3 majority gate of NOT, XOR and NOR. The reported structure designed with low complexity and smaller dimensions [18]. F. Parandin proposed a terahertz all optical NOR and AND logic gates with a bit rate of 1.54 Tbps. [19]. Saeed Olyaei et al. designed a high contrast ratio and ultra-compact size

all optical NOT & XOR gate. The data transmission rate calculated as 3.15 Tbps. [20]. Mohammad Mehdi Karkhanehchi et al. reported aX shaped optical half adder. [21]. Saleh Naghizade et al. proposed a ultra-fast optical analog to digital converter with a maximum response time of about 4 ps [22]. Saleh Naghizade et.al designed a all optical full adder with a maximum time delay of about 2.5 ps [23]. Amin Foroughifar et al. proposed a ring resonator based four channel optical filter with a maximum rise time of about less than 8ps [24]. Mojtaba Hosseinzadeh Sani et al. designed a ultra-narrowband all optical filter with less footprint of about 102.6  $\mu\text{m}^2$  [25]. Saleh Naghizade designed a linear defect based half adder which offers high contrast ratio and a low footprint as 16 dB and 158  $\mu\text{m}^2$  [26].

The encoders are primarily designed by different design mechanisms such as self-collimated effects [27], interference based defects [28], multimode interference effect [29], Mach Zehnder interferometer [30] and nonlinear Kerr effects [31]. By using the FDTD and PWE, contrast ratio, bit rate, response time and switching speed and footprint are examined. The encoder operated with self-imaging principle where the input profile introduced with different copies at regular intervals. Even though it offers low loss and wide bandwidth, it needs some precise control logic [32-35]. The present output depends on the phase of the input signals in addition to that a phase shifter required in self-collimation method [36-37]. Generally the ring resonator or waveguide based structure in encoders are designed with different waveguides such as T shape, L shape and Y shaped waveguides. The lattice used in the structure as square, hexagonal and triangular [38-47]. S. Naghizade, H. Khoshima designed all optical 4x2 encoder used triangular lattice low input power [28]. Ultra-compact, ultra-fast switching speed all optical 4x2 encoder based on photonic crystal is designed through square lattice with

proposed switching speed of 10 THz and contrast ratio of 7.1138 dB [29]. Siamak Gholamnejad and Mahdi Zavvari proposed 4x2 binary encoder using nonlinear resonant rings constructed by GaAs material and it reported switching threshold and time delay of about  $1\text{kW}/\mu\text{m}^2$  and 1ps respectively [30].

From the above literature analysis, the all optical encoders are designed with different techniques. High input power required for nonlinear materials. Though it has high contrast ratio it has some drawback such as temperature of the device will increase and the integration process is difficult. The linear materials offers low input power and switching speed will be high. Then the performances of the device will increase rapidly. The reported 4\*2 encoder designed by using a linear waveguide which offers better functional parameters such as contrast ratio, bit rate and delay time. Plane Wave Expansion (PWE) and Finite Difference Time Domain (FDTD) are two different numerical methods used to analyze the proposed encoder in order to calculate the band gap and output spectrum, respectively. The rest of the paper is organized as follows: Section 2 describes the structural designs and a simulation result of 4x2encoder is presented in Section III. Finally, Section IV concluded the proposed work.

## 2. Design of 4x2 encoder

The proposed structure designed with triangular lattice using silicon rods embedded in air. The number of rods in X and Z directions are 37 and 39, respectively. The refractive index, lattice constant and radius of rods in the proposed encoder are 3.45, 580nm and 116nm, respectively. Radius of rod is described by  $r=0.2*a$ , where  $a$  is lattice constant, which is defined as the distance between two rods. The proposed encoder is operated at 1520nm.

The point and line defects are used for guiding and controlling the signal propagation through waveguides. While removing a row or column of rods in a crystalline structure, the line defect introduced. Typically the encoder designed using OR logic gate function. Based on the OR gate logic function the proposed 4x2 encoder is designed using six waveguides. Fig. 1 shows logic circuit of 4x2 encoder design. It express that if any one input in activate, the output will be enabled. The four input waveguides of input ports are named as A, B, C, D and the two output waveguide as Y0 and Y1. The encoder is operated for four different logics as per the Table 1.

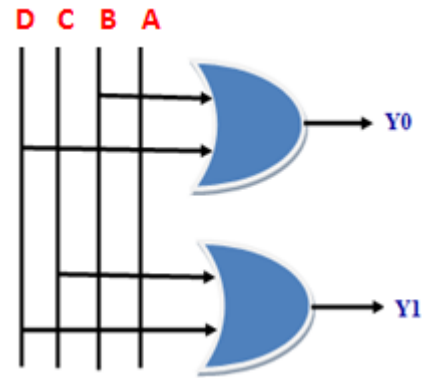


Fig. 1 Logic circuit of 4x2 encoder design (color online)

Table 1. 4\*2 Encoder Truth table

INPUT				OUTPUT	
A	B	C	D	Y0	Y1
1	0	0	0	0	0
0	1	0	0	1	0
0	0	1	0	0	1
0	0	0	1	1	1

To analyze the performance of proposed encoder, initially, the band structure is examined with the help of PWE method.

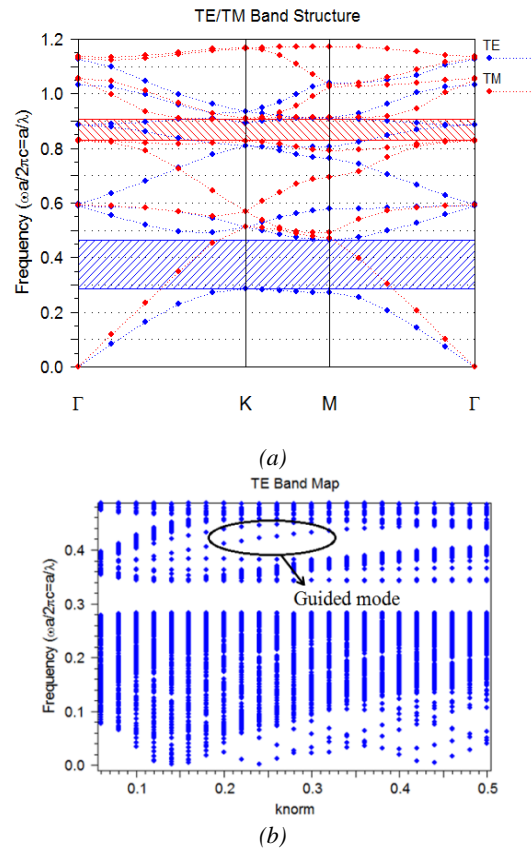


Fig. 2. (a) Band structure of photonic crystal and (b) Guided mode propagation (color online)

Both TE and TM PBG reported. The PBG is broken once line and point defect are created in the periodic structure and a guided mode is travelling inside it. Fig. 2(a) represented band structure of encoder before introducing defects in photonic crystal. The TE PBG is ranging from  $0.2860 < a/\lambda < 0.4639$ , and its corresponding wavelength in the range of  $1250\text{nm} < \lambda < 2027\text{nm}$  is observed. After the introduction of defects, the guided mode is propagated inside the PBG region. Fig. 2(b) demonstrates guided mode propagation in proposed 4x2 encoder design.

Fig. 3 (a) shows schematic structure of 4x2 encoder design with line and point defects. To design an input and output waveguide, the line defect introduced in the proposed structure. In order to enhance the power at the center of the output waveguide, a point defect incorporated in the proposed structure. The refractive index used as 3.45 and the radius of defect rod noted as 40 nm. In Fig. 3(b), 3D view of designed encoder is shown, in terms of the variation of rod radius in the vertical X direction. The footprint of proposed structure is  $415.84 \mu\text{m}^2$ .

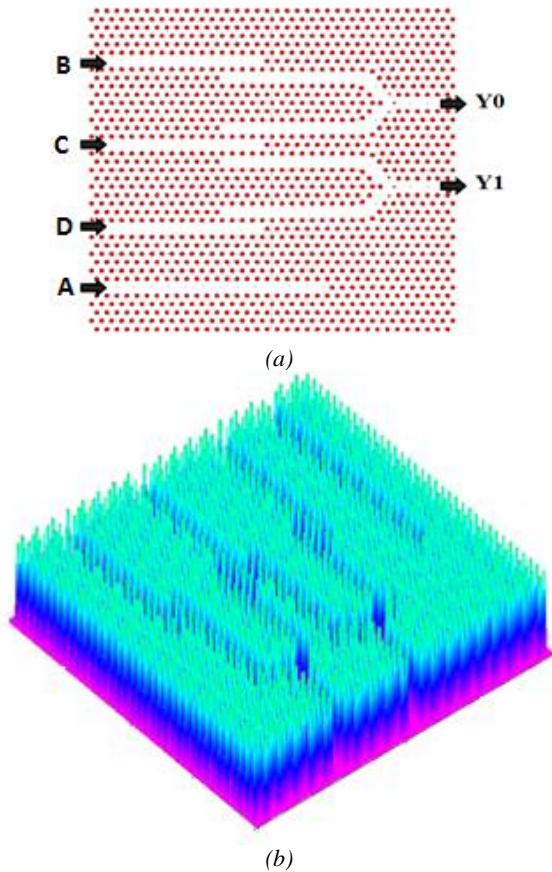


Fig. 3. (a) Schematic structure of proposed 4x2 encoder and (b) 3D structure (color online)

In center of Y shaped waveguides, the point defect created with 40 nm radius at refractive index 3.45, which is shown in Fig. 4. Three defect rods are incorporated in each Y shaped output waveguides to guide and confine the input signal which enable the desired output ports of encoder.

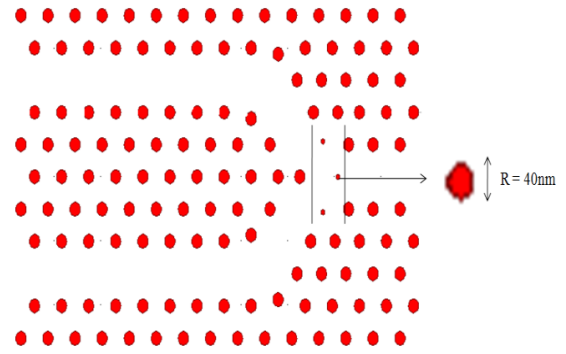


Fig. 4. Defect parts in proposed encoder (color online)

### 3. Result and discussion

The input signal with the power of 1mW is applied into the input port and the output power is measured using the following equation [11,12],

$$T(f) = \frac{1/2 \int \text{real}(p(f)^{\text{monitor}}) dS}{\text{SourcePower}} \quad (1)$$

In above equation (1), where  $T(f)$  denotes the normalized transmission as function of wavelength,  $p(f)$  is the represents pointing vector, and  $dS$  denotes the surface normal.

The Perfect Matched Layer (PML) is incorporated which is an artificial boundary layer to support the simulation in open boundary condition. It strongly absorbs the all incident waves in all directions, angle without any reflection inside the PC lattice [11, 12].

$$\Delta t \leq \frac{1}{c \sqrt{\frac{1}{\Delta X^2} + \frac{1}{\Delta Z^2}}} \quad (2)$$

In above equation (2), Where  $\Delta t$  denotes the step time, C represent the speed of light in free space, respectively. When the input power applied as 1mW and 0.7mW of power obtained at the output port.

The proposed 4x2 encoder is operated as per the logic given in Table 1. Based on logic function, concern output ports are activated. Figs. 5(a)-5(d) depict the signal propagation of the proposed 4x2 encoder. In four input waveguides, three input waveguides are connected in two Y shaped output waveguide and another one input waveguide is created separately in lattice structure for the reason of applying logic function of proposed structure. When input power is ON, the power coupled in output waveguides as described below.

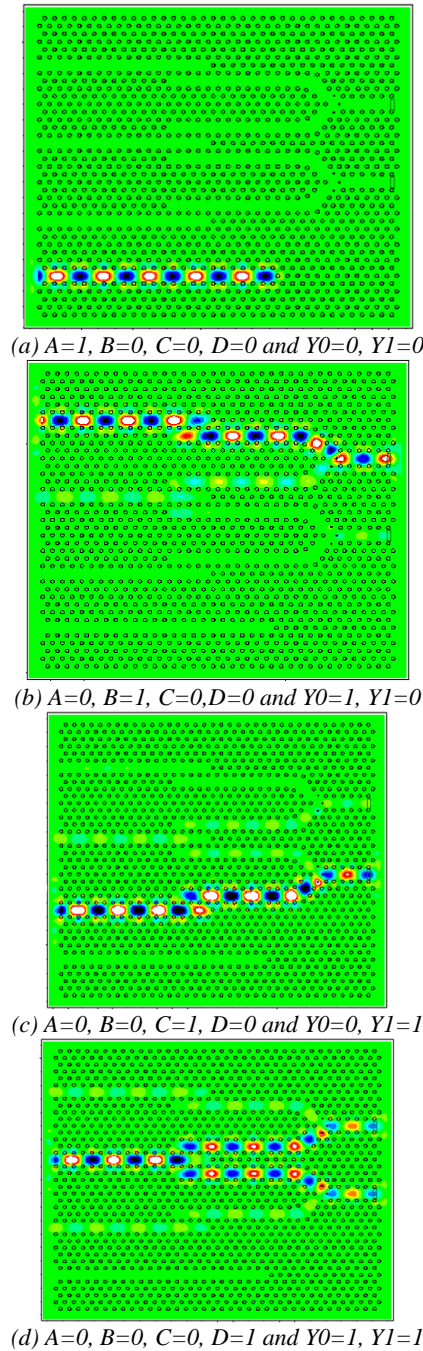


Fig. 5. Field distribution of 4x2 encoder design with different logics (a)  $A=1, B=0, C=0, D=0$  and  $Y0=0, Y1=0$ , (b)  $A=0, B=1, C=0, D=0$  and  $Y0=1, Y1=0$ , (c)  $A=0, B=0, C=1, D=0$  and  $Y0=0, Y1=1$  and (d)  $A=0, B=0, C=0, D=1$  and  $Y0=1, Y1=1$  (color online)

**Case 1:** When input A is ON i.e.,  $A=1$ , and B,C,D are OFF, the Gaussian input signal is not entered inside the waveguide, hence, there is no power obtained at the output port Y0 and Y1 as shown in Fig 5(a). The output power at  $Y0=0$  and  $Y1=0$ . Fig. 6(a) represents the corresponding field distribution when A is ON condition.

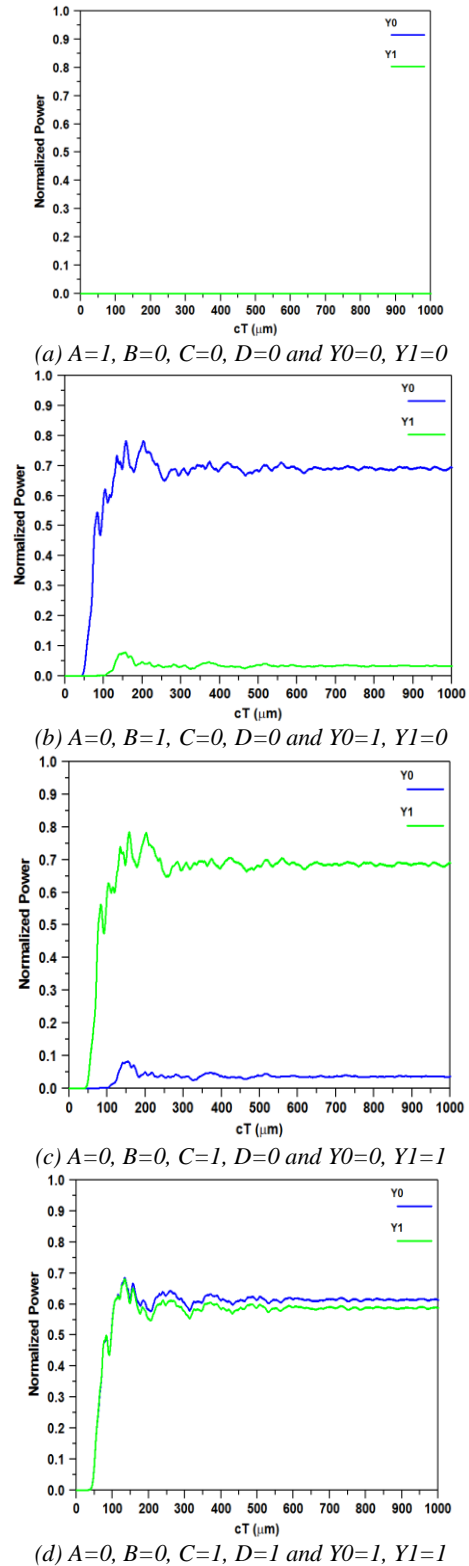


Fig. 6. Output response of proposed 4x2 encoder design (a)  $A=1, B=0, C=0, D=0$  and  $Y0=0, Y1=0$ , (b)  $A=0, B=1, C=0, D=0$  and  $Y0=1, Y1=0$ , (c)  $A=0, B=0, C=1, D=0$  and  $Y0=0, Y1=1$  and (d)  $A=0, B=0, C=0, D=1$  and  $Y0=1, Y1=1$  (color online)

**Case 2:** When B input is ON and A, C, D are OFF state, the input signal is passed to the input port B, the signal is propagating into the Y shaped waveguide. So, the output

port Y0 is ON, Around 70% of power reaches at the output port Y0 and remaining 3 % power reached at the output port Y1. Fig. 5(b) represents the signal propagation for 0100 and its corresponding output response curve depicts in Fig. 6(b).

**Case 3:** When input port C=1, and A=0, B=0, D=0. The input power applied to port D, at the center of the waveguide where the power coupled inside the waveguide. The corresponding field distribution represents in Fig. 5(c). The output port Y1 is ON, because C input port is connected to second Y shaped output waveguide. In this condition also the encoder is delivered maximum power to output port Y0 is 3% and Y1 is 70%.The respective output curve for logic 1101 is illustrated in Fig. 6(c).

**Case 4:** When input D is ON and other input ports such as A=0, B=0, C=0, the input signal entered into both of the Y shaped waveguide at resonant condition. Therefore, both output ports Y0 and Y1 are ON. D port of input waveguide is created in between of two Y shaped output waveguide. So, both of the output ports are enabled and it provides

maximum output power of above 50% in Y0 and Y1.The signal propagation for logic 0001 is shown in Fig. 5(d) and the output response curve displayed in Fig. 6(d).

For different logic combination, the simulation of signal propagation is providing analytical graph with normalized power versus time. Normalized power is described as maximum power to reach the device by desired input level of different combination. The system is taken time to send the signal from source to destination is referred as response time of the device.

The contrast ratio is calculated by taking logarithmic function of logic 1 and logic 0 values. The output power for logic 1 is 70% and logic 0 for 3%. Contrast ratio (CR) is defined as ratio of power at logic 1 and logic 0 with logarithmic function of  $CR=10\log(P_{ON}/P_{OFF})$ .The contrast ratio is 13.6dB. The response time of 0.28ps which is determined from  $t=0.194$  ps,  $t_1=0.2659$  and  $t_2=0.0712$  ps. The bit rate is 3.5 Tbps that is obtained from response time. And the parameter value is described in Table 2.

Table 2. Proposed 4\*2 encoder output, contrast ratio, response time and bit rate for different inputs

Input				Output		Output Power Level	Contrast Ratio	Response Time	Bit Rate
A	B	C	D	Y1	Y2	PON(PIn), POFF(POut)	PON / POFF		
1	0	0	0	0	0	0.70P <sub>in</sub>		0.28ps	3.5Tbps
0	1	0	0	0.70	0.03	0.03P <sub>Out</sub>	13.6dB		
0	0	1	0	0.03	0.70	0.58P <sub>in</sub>			
0	0	0	1	0.58	0.59	0.03P <sub>Out</sub>	12.86dB		

The impact of the functional parameters such as, contrast ratio, response time, Bit rate and normalized power of the proposed encoder with respect to the inner rod radius are analyzed and it is displayed in Figs. 7(a)-7(c). The inner rod radius is kept as 40nm as the maximum output power

70% is attained (See in Fig. 7(a)). It is also noticed that better response time of 0.28ps, contrast ratio of 13.6dB and 3.5Tbps of bit rate obtained (See in Figs. 7(b) &7(c)) at 40nm of inner rod radius.

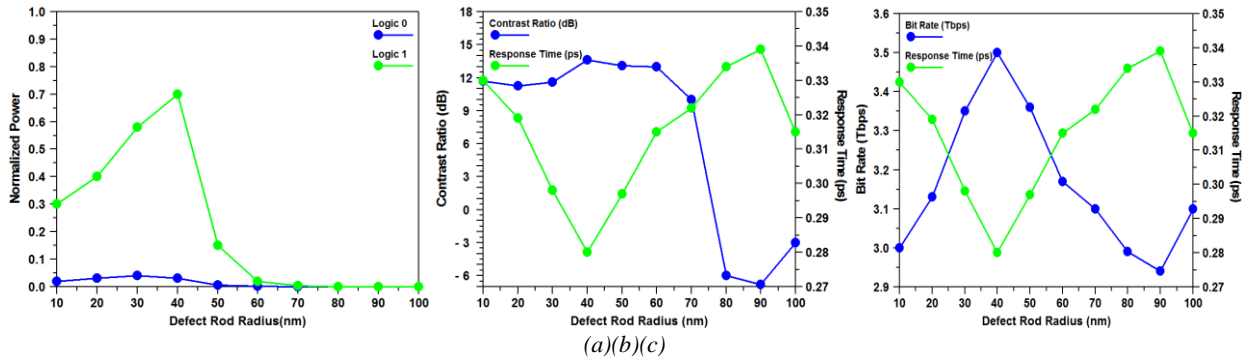


Fig. 7. (a) Impact of normalized power (b) Contrast ratio and response time and (c) Response time and bit rate with respect to the defect rod radius (color online)

The functional parameter of the proposed encoders is compared with the reported encoders which are listed in Table 3. From the table, it is clearly identified that the response time is decreased when the contrast ratio is high and vice versa. Alternatively, if the bit rate increases it limits both response time and contrast ratio. In addition, the size of the encoder is larger, when all the three parameters

are better. However, the proposed encoder provides significant enhancement in all the functional and structural parameters than the reported one. As the proposed encoder parameters are meeting the primary requirements for high speed optical integrated circuits, it could be considered for real time applications.

Table 3. Functional parameters comparison of proposed encoders with reported encoders

References	Type	Lattice	Defects	Footprint	Contrast Ratio (dB)	Response Time (ps)	Bit Rate (Tbps)
[38]	4*2	Square	Ring resonator	***	9.2	1.8	0.5
[42]	4*2	Square	Ring resonator	***	***	1	1
[44]	4*2	Square	Line and Point	880 $\mu\text{m}^2$	***	0.2	5
[48]	4*2	Triangular	Line and Point	***	***	5	0.2
[49]	4*2	Square	Ring resonator	128.52 $\mu\text{m}^2$	7.11	0.1	10
[50]	4*2	Square	Ring resonator	***	11.5	***	***
Proposed work	4*2 Encoder	Triangular	Line and Point	415.84 $\mu\text{m}^2$	13.6	0.28	3.5

#### 4. Conclusion

In this attempt, 4x2 encoder is designed by hexagonal lattice with array of silicon rods which is concerted by air substrate. The defects are created in order to reduce the power loss and easily coupled output ports without any barrier in the signal propagation. It is operated at 1520nm. The proposed encoder is providing contrast ratio of 13.6 dB, response time of 0.28ps and the bit rate of 3.5Tbps. So, it is suitable for photonic integrated circuits and optical networks.

#### Acknowledgments

I would like to register sincere thanks to my co-authors who gave their helpful discussions and support of this work and extend my thanks to our institute Mount Zion College of Engineering and Technology.

#### References

- [1] Guilian Yi, Byeng D. Youn, Journal of Structural and Multidisciplinary Optimization **54**, 1315 (2016).
- [2] Hamed Alipour-Banaei, Farhad Mahdizadeh, Somaye Serajmohammadi, Journal of Modern Optics **62**(6), 430 (2014).
- [3] Mona Neisy, Mohammad Soroosh, Karim Ansari-Asl, Journal of Photon Network Communication **35**(2), 245 (2018).
- [4] Sivasindhu Masilamani, Samundiswary Punniakodi, Journal of Optics **49**, 168 (2020).
- [5] Venkatachalam Rajarajan Balaji, Mahalingam Murugan, Savarimuthu Robinson, Rangaswamy Nakkeeran, Journal of Optical and Quantum Electronics **49**, 198 (2017).
- [6] Walid Aroua, Fathi Abdel Malek, Shyqyri Haxha,

IEEE Journal of Quantum Electronics **50**(8), 633 (2014).

- [7] Hamed Pezeshki, Vahid Ahmadi, Journal of Theoretical and Application Physics **6**(12), (2012).
- [8] S. Robinson, R. Nakkeeran, Optical Engineering **51**(11), 114001 (2012).
- [9] T. Betsy Saral, S. Robinson, R. Arunkumar, Journal of Photonics and Optical Technology **2**(4), 1 (2016).
- [10] K. Rama Prabha, S. Robinson, Silicon **13**(10), 3521 (2021).
- [11] Jayson K. Jayabharathan, G. Subhalakshmi, S. Robinson, Journal of Optical Communication **39**(3), 1 (2018).
- [12] R. Arunkumar, T. Suganya, S. Robinson, Photonic Optical technology **3**(1), 30 (2017).
- [13] R. Rajasekar, K. Parameshwari, S. Robinson, Plasmonics **14**(6), 1687 (2019).
- [14] Sh. Maktoobi, Sh. Bahadori-Haghighi, Journal of IET Electronics Letters **51**(13), 1016 (2015).
- [15] Fariborz Parandin, Journal of Optics and Laser Technology **113**, 447 (2019).
- [16] Ahmad Mohebzadeh-Bahabady, Saeed Olyae, Journal of IET Optoelectron. **12**(4), 191 (2018).
- [17] Fariborz Parandin, Mitra Moayed, Journal for Light and Electron Optics **216**, 164930 (2020).
- [18] F. Parandin, M. R. Malmir, M. Naseri, A. Zahedi, Journal of Superlattices and Microstructures **113**, 737 (2018).
- [19] F. Parandin, M. M. Karkhanehchi, Journal of Superlattices and Microstructures **101**, 253 (2017).
- [20] S. Olyae, M. Seifouri, A. Mohebzadeh-Bahabady, M. Sardari, Journal of Optical and Quantum Electronics **50**, 385 (2018).
- [21] Mohammad Mehdi Karkhanehchi, Fariborz Parandin, Abdulhamid Zahedi, Journal of Photon Netw. Commun. **33**, 159 (2017).
- [22] S. Naghizade, H. Saghaei, Opt. Quantum Electron. **53**(3), 149 (2021).
- [23] S. Naghizade, H. Saghaei, Opt. Quantum Electron.

- 53**(3), 154 (2021).
- [24] A. Foroughifar, H. Saghaei, E. Veisi, *Opt. Quantum Electron.* **53**(2), 101 (2021).
- [25] M. Hosseinzadeh Sani, A. Ghanbari, H. Saghaei, *Opt. Quantum Electron.* **52**(6), 295 (2020).
- [26] S. Naghizade, H. Saghaei, *Journal of Applied Research in Electrical Engineering* **1**(1), 1 (2020).
- [27] Yuanliang Zhang, Yao Zhang, Baojun Li, *Optics Express* **15**(15), 9287 (2007).
- [28] Nirmala Maria D'Souza, Vincent Mathew, *Optics and Laser Technology* **80**, 214 (2016).
- [29] Chunrong Tang, Xinyu Dou, Yuxi Lin, Hongxi Yin, Bin Wu, Qingchun Zhao, *Optics Communication* **316**(1), 49 (2014).
- [30] Alejandro Martínez, Pablo Sanchis, Javier Marti, *Optical and Quantum Electronics* **37**, 77 (2005).
- [31] Aryan Salmanpour, Shahram Mohammadnejad, Pedram Taghinejad Omran, *Optical and Quantum Electron.* **47**(12), 3689 (2015).
- [32] N. Saidani, W. Belhadj, F. AbdelMalek, *Optical and Quantum Electronics* **47**(7), 1829 (2015).
- [33] Aryan Salmanpour, Shahram Mohammadnejad, Ali Bahrami, *Optical and Quantum Electronics* **47**, 2249 (2015).
- [34] Debao Zhang, GuanJun You, *Physica E: Low-dimensional Systems and Nanostructures* **127**, 114469 (2020).
- [35] E. H. Shaik, N. Rangaswamy, *Journal of Opto-Electronics Review* **26**(1), 63 (2018).
- [36] Yuan Liang Zhang, Yao Zhang, Baojun Li, *Journal of Optics Express* **15**(15), 9287(2007).
- [37] H. Alipour-Banaei, M. G. Rabati, P. Abdollahzadeh-Badelbou, F. Mehdizadeh, *Physica E: Low dimensional Systems and Nanostructures* **75**, 77 (2016).
- [38] Hamed Seif-Dargahi, *Photonic Network Communications* **36**(2), 272 (2018).
- [39] Tamer A. Moniem, *J. of Modern Optics* **63**(8), 735 (2015).
- [40] ImanOuahab Rafah, *Optik* **127**(19), 7835(2016).
- [41] S. Neghizade, H. Khoshsima, *Optics Communications* **42**(1), 17 (2021).
- [42] Siamak Gholamnejad, Mahdi Zavvari, *Optical Quantum Electron.* **302**(49), (2017).
- [43] Mahdi Hassangholizadeh-Kashtiban, Reza Sabbaghi-Nadooshan, HamedAlipour-Banaei, *Optik* **126**(20), 2368 (2015).
- [44] Farhad Mehdizadeh, Mohanmmad Soroosh, Hamed Alipour-Banaei, *IET Optoelectronics* **11**(1), 29 (2017).
- [45] Yi-Pin Yang, Kuen-Cherng Lin, Chen Yang, Kun-Yi Lee, Wei-Yu Lee, *Journal of Optics* **142**, 354 (2017).
- [46] Amir Salimzadeh, Hamed Alipour-Banaei, *Optics Communications* **410**, 793 (2018).
- [47] Fatemeh Hadadan, Mohammed Soroosh, *Journal of Optics and Photonics* **13**(2), 119 (2019).
- [48] Ramin Yaghoobi, Sahel Javahernia, *Journal of Optical Communication* **42**(3), 425 (2021).
- [49] Tamer S. Mostafa, Nazmi A. Mohammed, El-Sayed M. El-Rabaie, *Journal of Computational Electronics* **17**(1), 1 (2018).
- [50] S. Monisha, D. Saranya, A. Rajesh, *Optical and Quantum Electronics* **51**(1), 1 (2018).

---

\* Corresponding author: lathakannan3945@gmail.com